Journal of Magnetic Resonance 306 (2019) 48–54

Contents lists available at ScienceDirect

Journal of Magnetic Resonance

journal homepage: www.elsevier.com/locate/jmr

The evolution of solution state NMR pulse sequences through the 'eyes' of triple-resonance spectroscopy

Lewis E. Kay *

Departments of Molecular Genetics, Biochemistry and Chemistry, The University of Toronto, Toronto, Ontario M5S 1A8, Canada
Hospital for Sick Children, Program in Molecular Medicine, 555 University Avenue, Toronto, Ontario M5G 1X8, Canada

ARTICLE INFO

Article history:
Received 18 January 2019
Revised 20 February 2019
Accepted 8 July 2019
Available online 12 July 2019

Keywords:
HNCA
HNCACB
Pulse sequences
Solution NMR

ABSTRACT

Careful pulse sequence design and optimization is critical to the success of a given NMR experiment. Over the past several decades the level of sophistication of NMR pulse sequences has increased tremendously, leading to large spectral sensitivity and resolution improvements, to data sets with far fewer artifacts, and to much more rapid acquisition times, opening up a wide range of applications. Here I briefly highlight how pulse sequence 'engineering' has evolved, focusing on liquid state NMR, and, in particular, on the HNCA-class of triple-resonance experiment. In many respects, the evolution of triple-resonance NMR mirrors the evolution of solution state NMR experiments in general, with 'tricks' that first appeared in triple-resonance pulse sequences or that were motivated by them now incorporated into a broad range of experiments.

1. Introduction

When asked to write a perspective on solution NMR spectroscopy to help celebrate the 50th anniversary of the Journal of Magnetic Resonance I was overwhelmed by the task. How can one possibly bridge all of the different areas of this ever-evolving field – from biomolecules to non-biological compounds, from proteins and nucleic acids to small molecules and metabolites, including all of the multitude of different experimental strategies and the plethora of processing approaches which, of course, are evolving constantly? The wide expanse of solution NMR that we its practitioners have nurtured over the years, and, in turn, has equally well met our scientific needs makes it truly challenging to do justice to this field in a few journal pages. I searched, therefore, for a common thread that might connect some of the different areas. Not surprisingly there are many, but perhaps the most obvious is the fact that each unique solution NMR application is driven by a pulse sequence [1–3] (often many) and that there is a direct correlation between the success of an experiment and the care invested in the design and optimization of the underlying pulse scheme. In this short monograph I want, therefore, to focus on pulse sequences and in particular on their design and optimization, highlighting an area of solution NMR that has been of longstanding interest to many in the community whose research involves the study of biomolecules. I will discuss only a small number of experiments, however, emphasizing how they have evolved over the years, highlighting new concepts that were introduced along the way and old ideas and myths that were gradually replaced over time. Often the insights obtained through the years in one area of NMR have implications in other branches of the technology and this is especially the case for solution triple-resonance, multidimensional NMR [4] that I will highlight here where developments in heteronuclear ^{1}H-X NMR [5–7] proved critical for the success of the solution NMR triple-resonance approach, that in turn influenced subsequent applications both in the solution and the solid state arenas.

2. Pulse sequence design: the importance of constantly getting better

Pulse sequence optimization has been critical to the success of the NMR field in general, and although this is perhaps most apparent in applications that would absolutely fail without careful experiment design it is also the case that even simple NMR pulse schemes can be improved. This point was made early on in the development of solution NMR spectroscopy in the context of a 'simple' pulse-acquire experiment where there is seemingly little to optimize. However, in a classic paper Ernst and Anderson showed over a half century ago that it is important to consider the longitudinal relaxation times (T_1) of the spins of interest rela-

* Address: Departments of Molecular Genetics, Biochemistry and Chemistry, The University of Toronto, Toronto, Ontario M5S 1A8, Canada.
E-mail address: kay@pound.med.utoronto.ca

https://doi.org/10.1016/j.jmr.2019.07.035
1090-7807/

tive to the time between pulses (T) to achieve optimal signal-to-noise [8]. The solution was to use an excitation pulse that flips the spins by an angle θ_E, termed the Ernst angle, which satisfies the relation $\cos\theta_E = e^{-T/T_1}$. This idea has been revisited in the design of certain classes of bio-based multi-dimensional experiments [9].

The evolution of triple-resonance NMR pulse schemes for studies of proteins has also followed a trajectory of improvements over the years that has significantly impacted on the utility of this class of experiment in studies of biomolecules of ever-increasing complexity. Perhaps this is best illustrated by considering a single pulse scheme and following it as it evolved over a period of more than a decade. In what follows I will consider, primarily, the HNCA sequence [10,11] although additional examples will be included to make important points. In the HNCA $^1H^N$ and ^{15}N nuclei are correlated with $^{13}C^\alpha$ spins belonging to the same residue and from the proceeding residue via magnetization transfer elements that exploit the heteronuclear scalar couplings [12] illustrated in Fig. 1. Thus, spectra are generated containing peaks at frequencies of ($^{13}C^{\alpha(jj-1)}$, $^{15}N^j$, $^1H^{Nj}$), providing both intra- and inter-residue connectivities.

Fig. 1 illustrates one of the earliest HNCA experiments, developed by Bax and coworkers, for studies of proteins that are uniformly ^{15}N, ^{13}C labeled [10,11]. Similar triple-resonance pulse schemes were proposed at about the same time by Montelione and Wagner who were pioneers in this area [13], but because their initial applications were illustrated on peptides optimization to the more challenging case of proteins was not required and experiments were recorded in 2D mode. Detailed explanations of all of the schemes presented here can be found in the original literature and in reviews [14] and textbooks [3,15]. A cogent discussion of the initial HNCA pulse sequence is given here, however, to emphasize the flow of magnetization transfer to those less familiar with triple-resonance NMR and to provide the necessary reference by which to understand subsequent improvements in experiments over time. My goal, in general, is to highlight only interesting nuances of each experiment, illustrating what the motivations were, how some of the important ideas introduced close to 30 years ago are still pervasive today and how, in some cases, pulse sequence elements have changed considerably, reflecting an increased understanding of how the spin physics must be optimized in applications to complex biomolecules. The pulse scheme of Fig. 1 can be understood in terms of the following magnetization transfers,

$$^1H^N \xrightarrow{^1J_{HN}} {}^{15}N(t_1) \xrightarrow{^1J_{NC\alpha},{}^2J_{NC\alpha}} {}^{13}C^{\alpha(jj-1)}(t_2) \xrightarrow{^1J_{NC\alpha},{}^2J_{NC\alpha}} {}^{15}N \xrightarrow{^1J_{HN}} {}^1H^N(t_3) \quad (1)$$

where the operative scalar couplings are indicated above the arrows denoting the transfers and the delays t_i are acquisition periods. It is noteworthy that immediately after the t_1 period ^{15}N transverse magnetization, anti-phase with respect to the attached amide proton, evolves with respect to its one- and two-bond scalar coupled $^{13}C^\alpha$ spins during the subsequent δ delay, which is chosen to optimize the transfer from ^{15}N to $^{13}C^\alpha$. The delay δ must also be selected to ensure that ^{15}N magnetization remains anti-phase with respect to the one-bond coupled amide proton spin, constraining it to a multiple of $1/J_{HN}$. Immediately prior to the first pair of simultaneous ^1H and $^{13}C^\alpha$ pulses that precede recording of $^{13}C^\alpha$ chemical shift (point A) the magnetization of interest can be written as $4I_ZN_{X,Y}C_Z^{\alpha(j)}/4I_ZN_{X,Y}C_Z^{\alpha(j-1)}$ where I have used the product operator notation [16,17] where L_j refers to the $j \in \{X, Y, Z\}$ component of L magnetization. The stage is now set to create triple spin terms $4I_YN_{X,Y}C_Y^{\alpha(j)}/4I_YN_{X,Y}C_Y^{\alpha(j-1)}$ that then evolve during the subsequent $^{13}C^\alpha$ chemical shift evolution period. The corresponding shift evolution of amide ^1H and ^{15}N magnetization is refocused during this interval by application of a simultaneous $^1H/^{15}N$ 180° pulse pair without concern for J_{HN} scalar coupled evolution as there is none for the double/zero quantum, $2I_YN_{X,Y}$, elements [15]. Subsequently, magnetization is transferred back to ^1H for detection, reversing the transfer steps of the initial part of the sequence. The triple-spin construct ($4I_YN_{X,Y}C_Y^\alpha$) is an interesting one and was designed to minimize the number of pulses in the experiment as it was felt that fewer pulses would require fewer phase cycling steps and hence generate less artifacts. Since time-consuming 3D data sets were recorded, minimization of phase cycling was an important consideration and often still is today, although the popularization of pulsed field gradient approaches (see below), originating with the work of Hurd and colleagues [18], has significantly reduced phase cycling requirements. It is of interest to note that relaxation and how it might influence the sensitivity of the experiment was not considered in this early design, although as I document below this subsequently become a focus.

Minimization of the number of pulses in the design of complex experiments continues to be important and I next consider an example that illustrates this point. Fig. 2 compares a pair of HA(CA)NNH pulse schemes [19], the first where the number of pulses is not minimized and the second where, using the principle of concatenation [19], the number of pulses is reduced considerably. The magnetization transfer pathway in the HA(CA)NNH can be described succinctly as

$$^1H^{\alpha(jj-1)}(t_1) \xrightarrow{^1J_{HC}} {}^{13}C^{\alpha(jj-1)} \xrightarrow{^1J_{NC\alpha},{}^2J_{NC\alpha}} {}^{15}N^j(t_2) \xrightarrow{^1J_{HN}} {}^1H^{Nj}(t_3) \quad (2)$$

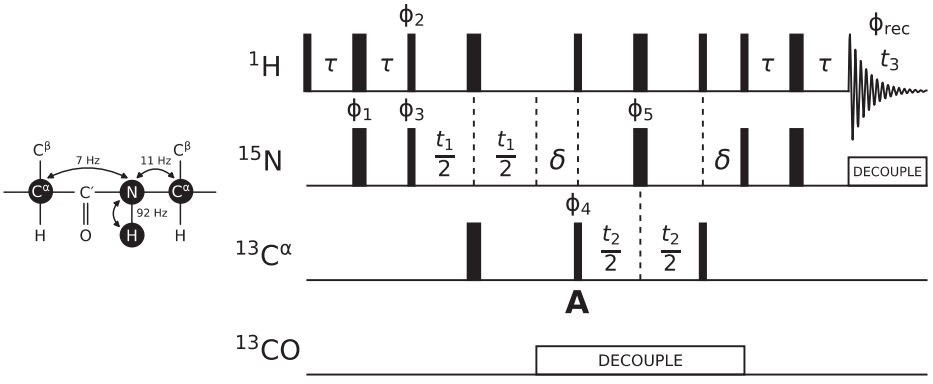

Fig. 1. Original 3D-HNCA pulse scheme, designed to minimize the number of pulses in the experiment. The nuclei that are correlated in the 3D data set are shown in the schematic to the left of the sequence, along with the magnetization transfer pathway and the magnitude of the scalar couplings that are involved. Spins whose chemical shifts are recorded are highlighted by black circles. Details can be found in the original Ref. [11].

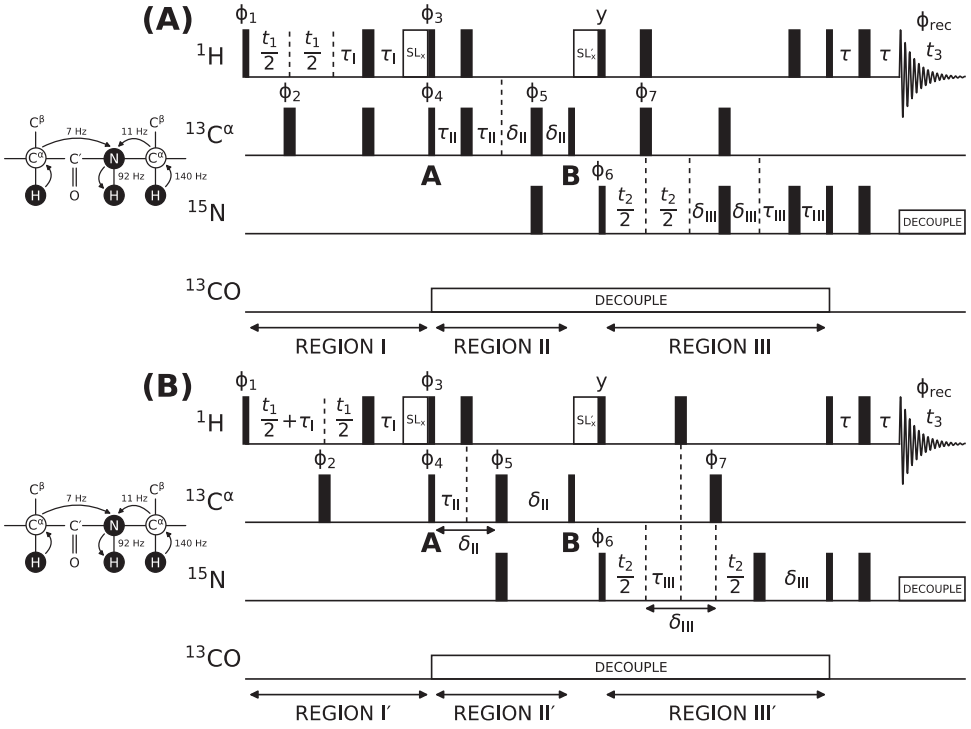

Fig. 2. Optimization of complex triple-resonance pulse sequences using the principle of concatenation. A triple-resonance experiment correlating $^{1}H^{\alpha}$, ^{15}N and $^{1}H^{N}$ chemical shifts is illustrated, focusing on non-concatenated (A) and concatenated (B) versions [19].

with the resulting 3D data set comprised of pairs of linked correlations at frequencies of $(\omega_{H^{\alpha(jj-1)}}, \omega_{N^{j}}, \omega_{H^{Nj}})$. The sequences of Fig. 2 are conveniently split into three regions that benefit from concatenation and in what follows we briefly illustrate the concept by considering regions II and III. Consider first region II (points A to B) where $^{13}C^{\alpha}$ magnetization evolves so as to effect the subsequent transfer to ^{15}N, $2C_{Y}^{\alpha(jj-1)}I_{Z} \rightarrow 2C_{Y}^{\alpha(jj-1)}N_{Z}$. Two critical steps occur during this interval: (i) refocusing of $^{13}C^{\alpha}$ magnetization, anti-phase with respect to the one-bond coupled $^{1}H^{\alpha}$ spin and (ii) defocusing of $^{13}C^{\alpha}$ magnetization from one- (intra-residue) and two- (inter-residue) bond ^{15}N-$^{13}C^{\alpha}$ scalar couplings. This occurs sequentially in the scheme of Fig. 2A (region II), but simultaneously in Fig. 2B (region II′), where the net evolution from J_{HC} is given by the relation

$$-\{-\boldsymbol{\tau}_{II} + (\boldsymbol{\delta}_{II} - \boldsymbol{\tau}_{II})\} + \boldsymbol{\delta}_{II} = 2\boldsymbol{\tau}_{II} = \frac{1}{2J_{HC}}. \quad (3)$$

Eq. (3) was derived by recognizing that, in general, the phase accrued by magnetization resulting from chemical shift or scalar coupled evolution during an interval of duration ζ is proportional to ζ. When a 180° pulse is applied to a spin that evolves due to chemical shift the resulting phase accrued is inverted, as it is when a single 180° pulse is applied to one or the other (not both) of the scalar coupled evolving spins [15]. Thus, focusing on region II′ of Fig. 2B and starting from point A, evolution of $^{13}C^{\alpha}$ magnetization from J_{HC} leads to a phase proportional to $\boldsymbol{\tau}_{II}$ and the subsequent application of a ^{1}H 180° pulse inverts the phase, which then evolves for an additional period of $\boldsymbol{\delta}_{II} - \boldsymbol{\tau}_{II}$ before the phase is further inverted by the $^{13}C^{\alpha}$ pulse in the center of the region II′. Finally, the phase evolves for a further delay of $\boldsymbol{\delta}_{II}$, with a net effective duration of scalar coupled evolution given by Eq. (3). The value of $2\tau_{II}$ is thus set to $1/(2J_{HC})$ for maximum sensitivity. Evolution of $^{13}C^{\alpha}$ magnetization due to $J_{NC\alpha}$ proceeds for the complete duration $2\delta_{II}$ as $^{13}C^{\alpha}$ and ^{15}N pulses are applied simultaneously at the midpoint of this interval. An optimal value for δ_{II} must be calculated, taking into account $^{13}C^{\alpha}$ transverse relaxation, as well as the fact that both one- (10–11 Hz [20]) and two- (6–8 Hz [20]) bond ^{15}N-$^{13}C^{\alpha}$ couplings are operative. Finally, $^{13}C^{\alpha}$ chemical shift evolution during region II′ is refocused by application of a $^{13}C^{\alpha}$ 180° pulse in the center of the evolution period.

Relations similar to Eq. (3) also exist for the evolution of ^{15}N magnetization during region III′. Following the logic described above it can be shown that the expressions

$$\begin{aligned} &-\{t_2/2 + \boldsymbol{\delta}_{III} + t_2/2) + \boldsymbol{\delta}_{III} = -t_2 \\ &-\{-(t_2/2 + \boldsymbol{\tau}_{III}) + (\boldsymbol{\delta}_{III} - \boldsymbol{\tau}_{III}) + t_2/2\} + \boldsymbol{\delta}_{III} = 2\boldsymbol{\tau}_{III} = \tfrac{1}{2J_{HN}} \\ &-\{-(t_2/2 + \boldsymbol{\delta}_{III}) + t_2/2\} + \boldsymbol{\delta}_{III} = 2\boldsymbol{\delta}_{III} \end{aligned} \quad (4)$$

are appropriate for evolution due to chemical shift, ^{1}H-^{15}N scalar couplings and ^{15}N-$^{13}C^{\alpha}$ scalar couplings, respectively. As for δ_{II} above, the value of δ_{III} must be optimized for maximum sensitivity by taking into account transverse relaxation of the ^{15}N spin and one- and two-bond ^{15}N-$^{13}C^{\alpha}$ scalar-coupled evolution.

The examples of concatenation described above exploit the evolution of several processes simultaneously, such as those arising from J_{HC} and $J_{NC\alpha}$ in region II′ of the HA(CA)NNH experiment. In many cases simultaneous evolution leads to significant sensitivity increases as well, as shown in the constant-time HNCA (CT-HNCA) pulse scheme of Fig. 3A [21]. The magnetization transfer pathway is similar to that in the version illustrated in Fig. 1. However, unlike the sequence of Fig. 1 where evolution of ^{15}N chemical shift occurs during a separate step that precedes the generation of anti-phase ^{15}N magnetization (with respect to C^{α}), $4I_{Y}N_{X,Y}C_{Y}^{\alpha(j)}/4I_{Y}N_{X,Y}C_{Y}^{\alpha(j-1)}$, in the scheme of Fig. 3A both chemical shift and ^{15}N-$^{13}C^{\alpha}$ scalar-coupled evolution occur simultaneously for a fixed, constant-time duration of $2T$ during which anti-phase ^{15}N magnetization with respect to spin I is not refocused (*i.e.*, $2T$ is a multiple of $1/J_{HN}$). Relative to the original experiment the signal intensity does not decrease as a function of t_1, leading to an increase in sensitivity that can be significant for applications to medium-large proteins. A second improvement in sensitivity is also possible through a sim-

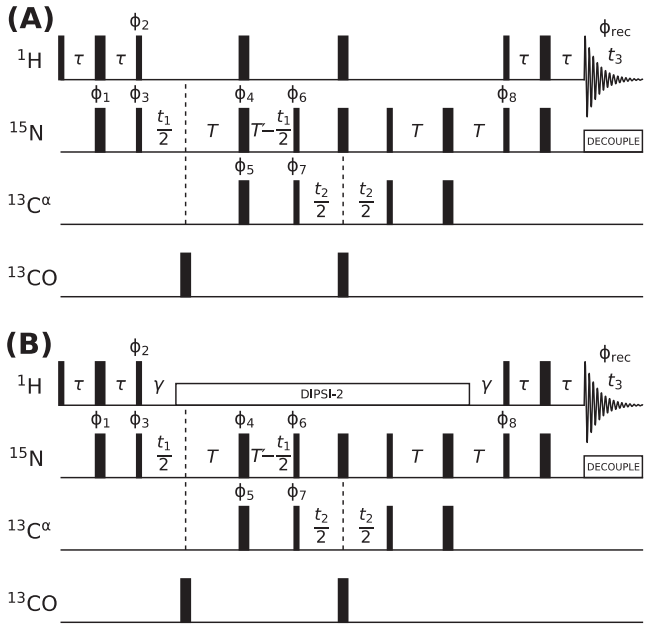

Fig. 3. Constant-time HNCA pulse schemes with simultaneous recording of ^{15}N chemical shift during evolution from $^{1,2}J_{NC\alpha}$ [21]. In (B) sensitivity is improved by refocusing anti-phase ^{15}N magnetization and maintaining it in-phase throughout the majority of the sequence using ^{1}H decoupling.

ple modification to the sequence. During both $2T$ (=22 ms) periods ^{15}N magnetization interconverts between anti-phase ($2N_YI_Z$) and in-phase (N_X) elements. For applications to protonated proteins, in particular, there is a significant imbalance in relaxation rates between $2N_YI_Z$ and N_X from cross-relaxation between amide proton I and neighboring proton spins that can significantly increase the effective relaxation rate of the anti-phase element, and hence decrease the sensitivity of the experiment [21,22]. In the scheme of Fig. 3B the delay γ is set to $1/(2J_{HN})$, allowing anti-phase ^{15}N magnetization to completely refocus immediately prior to the application of ^{1}H decoupling, thereby decreasing the effective transverse relaxation rates of the ^{15}N spins.

In many triple-resonance experiments pulses must be selective for specific regions of the ^{13}C spectrum, exciting either ^{13}CO or ^{13}C$^{\alpha}$ spins that resonate at ~175 and 55 ppm, respectively (see Fig. 3, for example). Initial applications made use of DANTE-type pulses involving a small number of elements with appropriate phases to achieve selective excitation [11] that were later improved upon by increasing the number of steps or by using shaped pulses that were designed to achieve selectivity. Many of the standard shaped pulses, such as those of the BURP variety [23], were rapidly incorporated into existing triple-resonance sequences, while other pulses such as SEDUCE-1 [24] were specifically developed with triple-resonance applications in mind. In other triple resonance applications pulses covering large bandwidths are required, such as when magnetization derived from the complete aliphatic ^{13}C spectral region must be inverted or refocused. It is often advantageous to use adiabatic pulses [25–28] in these cases that provide excellent inversion or refocusing, so long as pairs of pulses are employed in the case of refocusing, with essentially no dependence on rf power past a certain threshold. Considerable sensitivity gains can be realized in spectra that take advantage of such pulses, as demonstrated by Zweckstetter and Holak [29]. Adiabatic pulses have also assumed an increasingly important role in the context of broadband decoupling schemes [26], especially for studies at higher magnetic field strengths.

The triple-resonance pulse schemes illustrated in Figs. 1–3 rely on phase cycling to suppress artifacts due to pulse imperfections and off resonance effects and to ensure that the proper coherence transfer pathways are selected throughout the course of an experiment. The development of pulse field gradients proved very useful in this regard. Examples of the utility of pulsed field gradients for artifact suppression were provided by Bax and Pochapsky [30] in the context of a 3D CT-HN(CO)CA experiment in which correlations at frequencies of (^{15}N^{j},^{13}C$^{\alpha(j-1)}$,^{1}H^{Nj}) are obtained [21], Fig. 4. This experiment is similar to HNCA described above except that only inter-residue connectivities are provided, as the magnetization pathway involves transfer through the intervening ^{13}CO spin between ^{13}C$^{\alpha(j-1)}$ and the amide ^{15}N,^{1}H pair of residue j,

$$^{1}H^{Nj} \xrightarrow{^{1}J_{HN}} {}^{15}N^{j}(t_1) \xrightarrow{^{1}J_{NCO}} {}^{13}CO^{(j-1)} \xrightarrow{^{1}J_{C\alpha CO}} C^{\alpha(j-1)}(t_2) \times \xrightarrow{^{1}J_{C\alpha CO}} {}^{13}CO^{(j-1)} \xrightarrow{^{1}J_{NCO}} {}^{15}N^{j} \xrightarrow{^{1}J_{HN}} {}^{1}H^{Nj}(t_3). \quad (5)$$

Thus, the combined analysis of HN(CO)CA and HNCA data sets allows the unequivocal identification of intra- and inter-residue crosspeaks in the HNCA that simplifies the assignment process. Focusing on the new line in the timing diagram of Fig. 4 termed 'G_z' it can be seen that gradient g_1 defocusses transverse magnetization, retaining the desired two spin order element $2I_ZN_Z$, gradients g_2, g_3 and g_5 are applied when the magnetization of interest is transverse and serve to eliminate artifacts from imperfections in the refocusing pulses that they surround, and the gradient g_4 pair suppresses artifacts caused by imperfections in a ^{1}H 180° pulse that is applied to restrict J_{HN} scalar coupled evolution of ^{15}N magnetization to a total duration of $1/(2J_{HN})$ without effecting the chemical shift evolution of ^{15}N transverse magnetization.

The use of pulsed field gradients described above leads to artifact suppression and selection against certain unwanted coherence transfer pathways. It is also possible, however, to use gradients to actively select for coherence transfer pathways of interest. A number of experiments were initially proposed that achieved this goal and generated pure absorptive spectra but at the expense of a factor of $\sqrt{2}$ less sensitivity relative to 'standard' pulse schemes where gradients are not used for coherence selection [31–33]. However, by exploiting the elegant PEP (Preservation of Equivalent Pathways) approach of Rance and coworkers [34] it became possible to achieve sensitivity increases of factors of $\sqrt{2}$ and 2 relative to non-gradient schemes and 'first generation' gradient selection experiments, respectively [35,36]. Fig. 5 illustrates a gradient sensitivity enhanced HNCACB pulse scheme [37] that is similar to HNCA, described above, but includes an additional transfer step that enables recording both ^{13}C$^{\alpha}$ and ^{13}C$^{\beta}$ chemical shifts, so that cross peaks of the form (^{13}C$^{\alpha(j,j-1)}$+^{13}C$^{\beta(j,j-1)}$, ^{15}N^{j}, ^{1}H^{Nj}) are obtained [38]. The version of HNCACB illustrated in Fig. 5 increases sensitivity by (i) minimization of effective ^{15}N transverse relaxation rates through ^{1}H decoupling and by (ii) recording the data set in the sensitivity enhanced mode. Together these improvements help offset the approximate factor of 2 sensitivity decrease that is associated with recording both ^{13}C$^{\alpha}$ and ^{13}C$^{\beta}$ chemical shifts, relative to the standard HNCA pulse scheme.

Many of the triple-resonance experiments that are in standard use, and all of those that are based on sequences where the magnetization of interest originates on or is detected via amide protons, are recorded in $^{1}H_2O$ solvent. Because water proton T_1s are typically on the order of several seconds, significantly longer than the recovery delays that are used in standard multi-dimensional NMR experiments, the water resonance invariably becomes partially (or fully) saturated unless care is taken to prevent this. Further, because water proton T_1s are longer than amide proton T_1s in typical protein preparations, the saturation of water is readily transferred to amides via exchange and subsequently to other sites in the protein due to spin diffusion. The net result is signal attenuation. It is important to realize that there is a decrease in sensitiv-

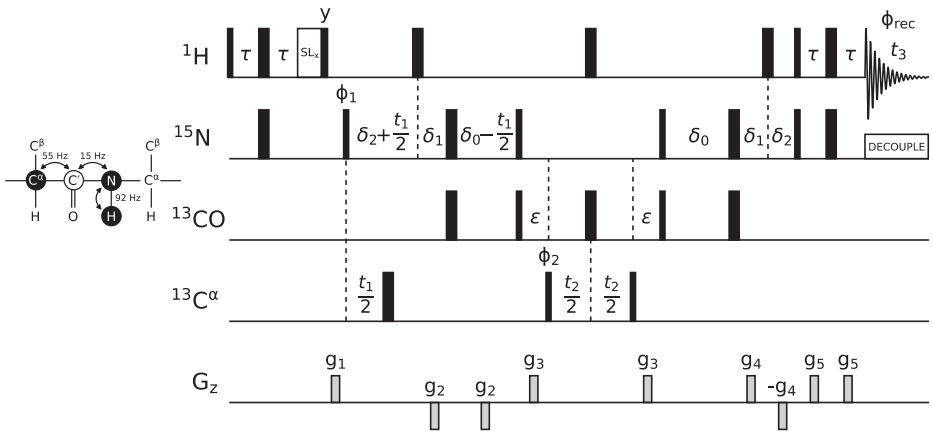

Fig. 4. An HN(CO)CA triple-resonance experiment, illustrating the use of pulsed field gradients to suppresses artifacts [30]. The magnetization transfer pathway is indicated to the left of the timing diagram.

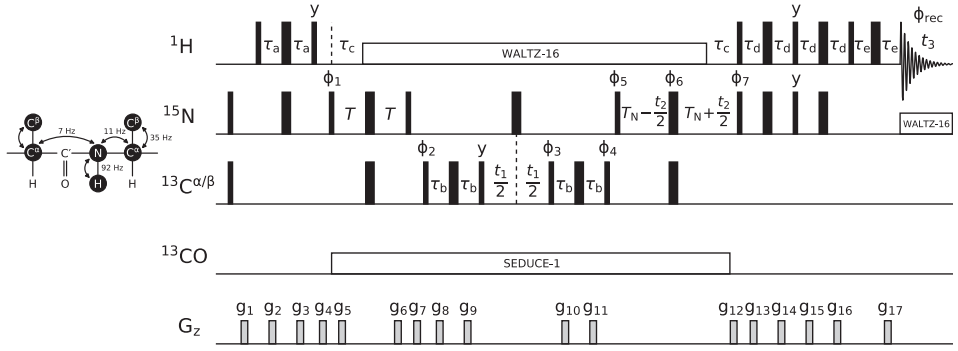

Fig. 5. An enhanced-sensitivity HNCACB pulse scheme using pulsed field gradients for coherence transfer selection [37]. The transfer of magnetization involved in the experiment is indicated in the schematic to the left of the timing diagram. Gradients are numbered sequentially from 1 to 17, as in the original reference, although many are applied as pairs (such as g_2 and g_3, for example) and have identical strengths and durations. Decoupling is interrupted during the application of gradients g5-g11.

ity even in experiments that do not involve the amide protons directly, mediated through exchange/NOE effects involving protons that exchange with water. Grzesiek and Bax showed that simple modifications to the pulse sequences of the day could be made involving the use of water selective pulses that restore magnetization to the +Z-axis at the completion of each scan, prior to the recovery period [39]. In this manner water magnetization can be largely preserved and thus used as a reservoir to replenish protein amide magnetization through solvent exchange during the recovery delay.

With the development of more robust experiments came the desire for applications to larger sized proteins. Fundamentally, triple-resonance experiments are limited by transverse spin relaxation during the (often) lengthy transfer steps, especially those involving transverse aliphatic ^{13}C magnetization where large dipolar interactions with attached protons lead to rapid signal decay [40]. A solution to the problem was found by replacing ^{13}C-bound protons with deuterons [41]. Although deuterons are spin 1, as opposed to spin ½ for protons, the gyromagnetic ratio of ^{2}H is approximately 6.5-fold smaller than that of ^{1}H, reducing the one-bond hydrogen-^{13}C dipolar relaxation interaction by close to 20-fold for ^{2}H. This advantage does come with the requirement of slightly more complex pulse schemes, however. Recall that in the absence of ^{2}H relaxation the ^{13}C spectrum of a ^{13}C–^{2}H spin-pair is a 1:1:1 triplet. ^{2}H spin relaxation interchanges the three ^{13}C multiplet components in a manner analogous to chemical exchange. However, the interchange is not sufficiently fast to self-decouple the triplet [42] so that to achieve narrowing of the ^{13}C line ^{2}H decoupling must be used [41]. With the development of higher field magnets and the concomitant increase in ^{2}H T_1 values this can be achieved easily and the sensitivity gains afforded by deuteration can be substantial, as first demonstrated by Bax and coworkers in an experiment that relays magnetization between sequential amides [41], and subsequently by the Kay laboratory who developed a family of 3D and 4D ^{2}H-based triple-resonance pulse schemes for studies of moderately high molecular weight proteins [43–45]. Other notable initial contributions in this area include the work of Venters, Farmer and colleagues [46,47]. Fig. 6 provides an example of an HNCA pulse scheme for studies involving deuterated proteins [48] that includes many of the features described such as water preservation (water selective pulses are indicated by the semi-oval shapes), as well as ^{13}C$^\beta$ and ^{2}H decoupling during the period where ^{13}C$^\alpha$ magnetization is transverse. It is straightforward to modify the experiment to get additional signal-to-noise through the enhanced sensitivity approach detailed above [14]. Note that ^{1}H $90_Y/90_{-Y}$ pulses flank the ^{1}H WALTZ16$_X$ decoupling elements so that complete decoupling cycles do not have to be used in order to ensure that the water magnetization remains minimally perturbed [49], a requirement that might be difficult to fulfill in a routine manner for many experiments. In our laboratory we prefer to include 90° ^{2}H flanking pulses surrounding the ^{2}H decoupling trains as well so as to place ^{2}H magnetization along the +Z-axis after decoupling that minimizes perturbation of the lock signal [47].

Minimization of relaxation losses during multi-step transfer experiments is critical, especially in applications involving high molecular weight proteins. Examples of how this can be accomplished have already been given, yet further improvements can

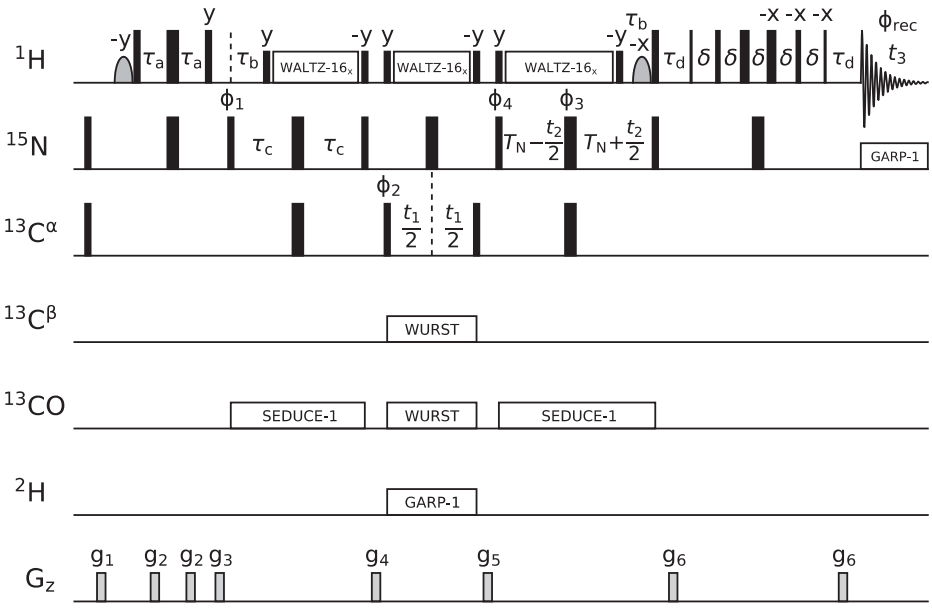

Fig. 6. HNCA pulse scheme for application to deuterated proteins with $^{13}C^{\beta}$ decoupling to improve spectral sensitivity and increase resolution in the $^{13}C^{\alpha}$ dimension [48].

be made. In this regard a major advance in NMR experiments for the study of biomolecules occurred with the development of TROSY-based pulse schemes [50], with particular benefits to triple-resonance applications [51,52]. Building on the fact that individual lines in an AX spin-system can relax very differently due to interference effects between two or more relaxation interactions [53,54], Pervushin, Wüthrich and coworkers illustrated the benefits of selecting for the slowly relaxing magnetization components in the case of backbone amide ^{1}H-^{15}N spin-pairs [50] (as well as in the aromatic ^{1}H–^{13}C spin system [55]). Thus even though only 50% of the net magnetization is preserved in the ^{1}H-^{15}N TROSY-scheme, in the absence of relaxation, the gains can be significant over non-TROSY experiments where fast and slowly relaxing amide components are mixed [51]. Desired multiplet components can be chosen with spin-state selective schemes that transfer magnetization from the slowly relaxing amide ^{15}N multiplet component to the narrow amide ^{1}H line using phase cycling, gradients or a combination of the two [56]. Careful experimental design is required to ensure that fast and slowly relaxing components are not mixed during the course of a pulse sequence. For example, ^{1}H 180° pulses interconvert TROSY and anti-TROSY ^{15}N lines, so that these should only be applied, where necessary, in pairs. A similar situation occurs for the ^{1}H lines, where a single ^{15}N 180° pulse converts the components as well. Interchange between ^{15}N TROSY and anti-TROSY lines can also result from cross relaxation between the amide proton of the ^{1}H-^{15}N spin-pair and neighboring proton spins. This can be minimized through the use of high levels of protein deuteration that is also important for attenuating ^{13}C relaxation, as discussed above. Fig. 7 illustrates a TROSY-HNCACB pulse scheme developed by Wüthrich and coworkers [57]. In comparison to the non-TROSY HNCACB of Fig. 5 the most striking difference is the absence of ^{1}H decoupling which efficiently mixes fast and slowly relaxing ^{15}N magnetization components, a situation that is not desired in studies of large proteins. As ^{15}N magnetization is transverse for approximately 50 ms in this experiment, retaining the ^{15}N TROSY component can lead to substantial gains in signal-to-noise. Additional, small gains in sensitivity can be obtained by optimization of the magnetization transfer pathway from ^{15}N to ^{1}H prior to detection, as described previously [58].

Sensitivity in triple-resonance applications is of great importance and, as described above, many different approaches ranging

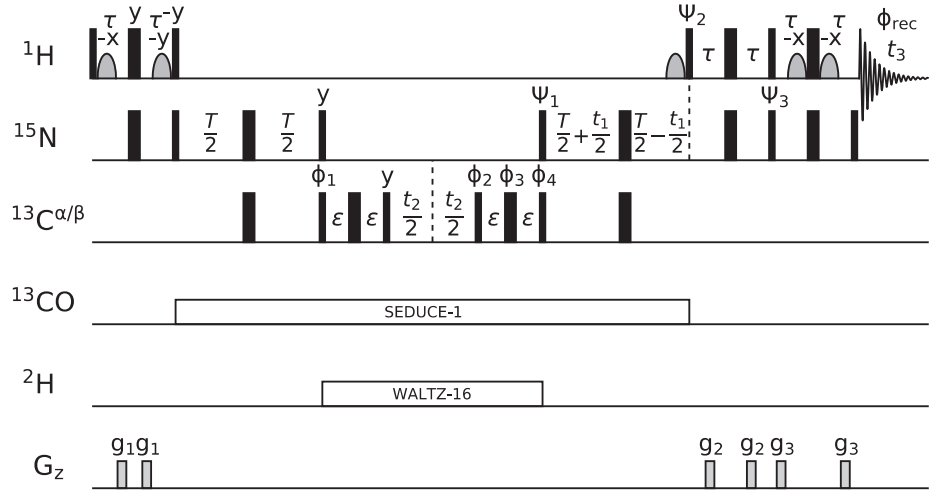

Fig. 7. A TROSY-based HNCAB pulse scheme that affords significantly improved sensitivity in applications involving high molecular weight proteins [57].

from pulse sequence design to isotope labeling schemes have been developed to address this issue. In this regard the minimization of water saturation during the course of an experiment, already mentioned in this article, is critical as this allows water to be used as a bath to rapidly restore longitudinal amide ^{1}H magnetization during the recovery delay between scans [39,49,59]. Water selective pulses can be used in a straightforward manner to ensure that water magnetization is 'controlled' throughout the pulse sequence and, in particular, placed along the +Z-axis at the end of each scan (Fig. 6, shaped ^{1}H pulses). Similarly, it is possible to execute amide-based triple-resonance experiments in a manner such that aliphatic proton magnetization remains largely unperturbed by the application of amide selective ^{1}H pulses, and, when necessary, by broad-banded pulses applied in pairs. Pervushin and coworkers have shown significant sensitivity gains with this elegant approach [60].

The significant reduction in effective amide ^{1}H T_1s from these so-called longitudinal relaxation optimized experiments [60] has important practical applications as well. In a series of impressive papers Brutscher's group has shown that it is possible to exploit the rapid recovery of proton polarization in order to expedite recording of potentially time-consuming 3D triple resonance data sets [61,62]. These so-called BEST pulse schemes have significant implications in studies of unstable proteins or in cases where kinetic data must be recorded in real time because high quality data sets can be obtained even when very short longitudinal recovery delays (100–200 ms) are used. When sensitivity permits, further decreases in recording times are possible, by the addition of non-uniform sampling, projection reconstruction, spatially encoded frequency labeling or GFT-spectroscopy methods [63].

3. Concluding remarks

In this brief monograph, highlighting the evolution of particular aspects of liquid-state pulse sequence design, I have chosen to focus on the HNCA-class of triple-resonance experiment to illustrate how, over a period of close to two decades, new ideas and insights have led to pulse schemes of ever-increasing sophistication. Although the focus has been on the HNCA here it is clear that the improvements extend beyond this class of experiment and, indeed, beyond the domain of triple-resonance NMR, impacting on virtually all solution state NMR experiments in some way. In part, the advances have been stimulated by instrumentation including shielded pulsed field gradient coils and higher magnetic fields. But equally important has been an increased understanding of spin physics and how to optimize experiments by taking into account simple rules that govern how magnetization evolves and relaxes during complex pulse sequences. This attention to detail and to basic NMR science has significantly increased both the types of questions that can now be addressed and the nature of the applications that are now possible.

Acknowledgements

This work was supported by grants from the Canadian Institutes of Health Research (CIHR) and the Natural Sciences and Engineering Research Council of Canada. L.E.K. holds a Canada Research Chair in Biochemistry. The author is grateful to Dr. Tairan Yuwen for preparation of figures and useful discussion.

References

[1] K. Wüthrich, NMR of Proteins and Nucleic Acids, John Wiley & Sons, New York, 1986.
[2] R.R. Ernst, G. Bodenhausen, A. Wokaun, Principles of Nuclear Magnetic Resonance in One and Two Dimensions, Oxford University Press, Oxford, 1987.
[3] J. Cavanagh, W.J. Fairbrother, A.G. Palmer, N.J. Skelton, Protein NMR Spectroscopy: Principles and Practice, Academic Press, San Diego, 1996.
[4] A. Bax, Curr. Opin. Struct. Biol. 4 (1994) 738–744.
[5] A. Bax, S.W. Sparks, D.A. Torchia, Methods in Enzymol. 176 (1989) 134–150.
[6] G. Wagner, D. Bruhwiler, Biochemistry 25 (1986) 5839–5843.
[7] S.W. Fesik, E.R. Zuiderweg, Q. Rev. Biophys. 23 (1990) 97–131.
[8] R.R. Ernst, W.A. Anderson, Rev. Sci. Instr. 37 (1966) 93–102.
[9] P. Schanda, E. Kupce, B. Brutscher, J. Biomol. NMR 33 (2005) 199–211.
[10] M. Ikura, L.E. Kay, M. Krinks, A. Bax, Biochemistry 30 (1991) 5498–5503.
[11] L.E. Kay, M. Ikura, R. Tschudin, A. Bax, J. Magn. Reson. 89 (1990) 496–514.
[12] V.F. Bystrov, Prog. NMR Spectrosc. 10 (1976) 41–81.
[13] G.T. Montelione, G. Wagner, J. Magn. Reson. 87 (1990) 183–188.
[14] M. Sattler, J. Schleucher, C. Griesinger, Prog. Nucl. Magn. Reson. Spectrosc. 34 (1999) 93–158.
[15] G.S. Rule, T.K. Hitchens, Fundamentals of Protein NMR Spectroscopy, Springer, 2006.
[16] O.W. Sorensen, G.W. Eich, M.H. Levitt, G. Bodenhausen, R.R. Ernst, Prog. NMR Spectrosc. 16 (1983) 163–192.
[17] F.J.M. Van de Ven, C.W. Hilbers, J. Magn. Reson. 54 (1983) 512–520.
[18] R. Hurd, J. Magn. Reson. 87 (1990) 422–428.
[19] L.E. Kay, M. Ikura, A. Bax, J. Magn. Reson. 91 (1991) 84–92.
[20] F. Delaglio, D.A. Torchia, A. Bax, J. Biomol. NMR 1 (1991) 439–446.
[21] S. Grzesiek, A. Bax, J. Magn. Reson. 96 (1992) 432–440.
[22] A. Bax, M. Ikura, L.E. Kay, D.A. Torchia, R. Tschudin, J. Magn. Reson. 86 (1990) 304–318.
[23] H. Geen, R. Freeman, J. Magn. Reson. 93 (1991) 93–141.
[24] M.A. McCoy, L. Mueller, J. Am. Chem. Soc. 114 (1992) 2108–2112.
[25] J. Baum, R. Tycko, A. Pines, J. Chem. Phys. 79 (1983) 4643–4644.
[26] E. Kupce, R. Freeman, J. Magn. Reson., Ser. A. 115 (1995) 273–276.
[27] M. Silver, R. Joseph, D. Holt, J. Magn. Reson. 59 (1984) 347–351.
[28] J.-M. Böhlen, I. Burghardt, M. Rey, G. Bodenhausen, J. Magn. Reson. 90 (1990) 183–191.
[29] M. Zweckstetter, T.A. Holak, J. Biomol. NMR 15 (1999) 331–334.
[30] A. Bax, S. Pochapsky, J. Magn. Reson. 99 (1992) 638–643.
[31] J.R. Tolman, J. Chung, J.H. Prestegard, J. Magn. Reson. 98 (1992) 462–467.
[32] A.L. Davis, E.D. Laue, J. Keller, D. Moskau, J. Lohman, J. Magn. Reson. 94 (1991) 637–644.
[33] J. Boyd, N. Soffe, B. John, D. Plant, R. Hurd, J. Magn. Reson. 98 (1992) 660–664.
[34] J. Cavanagh, M. Rance, Ann. Rep. NMR Spectrosc. 27 (1993) 1–58.
[35] L.E. Kay, P. Keifer, T. Saarinen, J. Am. Chem. Soc. 114 (1992) 10663–10665.
[36] J. Schleucher, M. Sattler, C. Griesinger, Angew. Chem. Int. Ed. Engl. 32 (1993) 1489–1491.
[37] D.R. Muhandiram, L.E. Kay, J. Magn. Reson. B 103 (1994) 203–216.
[38] M. Wittekind, L. Mueller, J. Magn. Reson. Ser. B 101 (1993) 201–205.
[39] S. Grzesiek, A. Bax, J. Am. Chem. Soc. 115 (1993) 12593–12594.
[40] D.T. Browne, G.L. Kenyon, E.L. Packer, H. Sternlicht, D.M. Wilson, J. Am. Chem. Soc. 95 (1973) 1316–1323.
[41] S. Grzesiek, J. Anglister, H. Ren, A. Bax, J. Am. Chem. Soc. 115 (1993) 4369–4370.
[42] R.E. London, D.M. LeMaster, L.G. Werbelow, J. Am. Chem. Soc. 116 (1994) 8400–8401.
[43] T. Yamazaki, W. Lee, C.H. Arrowsmith, D.R. Muhandiram, L.E. Kay, J. Am. Chem. Soc. 116 (1994) 11655–11666.
[44] T. Yamazaki, W. Lee, M. Revington, D.L. Mattiello, F.W. Dahlquist, C.H. Arrowsmith, L.E. Kay, J. Am. Chem. Soc. 116 (1994) 6464–6465.
[45] X. Shan, K.H. Gardner, D.R. Muhandiram, N.S. Rao, C.H. Arrowsmith, L.E. Kay, J. Am. Chem. Soc. 118 (1996) 6570–6579.
[46] R.A. Venters, B.T. Farmer, C.A. Fierke, L.D. Spicer, J. Mol. Biol. 264 (1996) 1101–1116.
[47] B.T. Farmer, R. Venters, J. Am. Chem. Soc. 117 (1995) 4187–4188.
[48] H. Matsuo, E. Kupce, H. Li, G. Wagner, J. Magn. Reson. 113 (1996) 91–96.
[49] L.E. Kay, G.Y. Xu, T. Yamazaki, J. Magn. Reson., Ser. A 109 (1994) 129–133.
[50] K. Pervushin, R. Riek, G. Wider, K. Wüthrich, Proc. Natl. Acad. Sci. USA 94 (1997) 12366–12371.
[51] M. Salzmann, K. Pervushin, G. Wider, H. Senn, K. Wuthrich, Proc. Natl. Acad. Sci. USA 95 (1998) 13585–13590.
[52] D. Yang, L.E. Kay, J. Am. Chem. Soc. 121 (1999) 2571–2575.
[53] M. Goldman, J. Magn. Reson. 60 (1984) 437–452.
[54] M. Gueron, J.L. Leroy, R.H. Griffey, J. Am. Chem. Soc. 105 (1983) 7262–7266.
[55] K. Pervushin, R. Riek, G. Wider, K. Wüthrich, J. Am. Chem. Soc. 120 (1998) 6394–6400.
[56] K.V. Pervushin, G. Wider, K. Wüthrich, J. Biomol. NMR 12 (1998) 345–348.
[57] M. Salzmann, G. Wider, K. Pervushin, H. Senn, K. Wuthrich, J. Am. Chem. Soc. 121 (1999) 844–848.
[58] D. Yang, L.E. Kay, J. Biomol. NMR 14 (1999) 273–276.
[59] J. Stonehouse, G.L. Shaw, J. Keeler, E.D. Laue, J. Mag. Reson. Ser. A 107 (1994) 178–184.
[60] K. Pervushin, B. Vogeli, A. Eletsky, J. Am. Chem. Soc. 124 (2002) 12898–12902.
[61] P. Schanda, H. Van Melckebeke, B. Brutscher, J. Am. Chem. Soc. 128 (2006) 9042–9043.
[62] Z. Solyom, M. Schwarten, L. Geist, R. Konrat, D. Willbold, B. Brutscher, J. Biomol. NMR 55 (2013) 311–321.
[63] R. Freeman, E. Kupce, J. Biomol. NMR 27 (2003) 101–113.